Audio-based Relative Positioning System for Multiple Micro Air Vehicle Systems

Meysam Basiri[1,2], Felix Schill [1], Dario Floreano[1] and Pedro U.Lima[2]

***Abstract*—Employing a group of independently controlled flying micro air vehicles (MAVs) for aerial coverage missions, instead of a single flying robot, increases the robustness and efficiency of the missions. Designing a group of MAVs requires addressing new challenges, such as inter-robot collision avoidance and formation control, where individual's knowledge about the relative location of their local group members is essential. A relative positioning system for a MAV needs to satisfy severe constraints in terms of size, weight, processing power, power consumption, three-dimensional coverage and price. In this paper we present an on-board audio based system that is capable of providing individuals with relative positioning information of their neighbouring sound emitting MAVs. We propose a method based on coherence testing among signals of a small onboard microphone array to obtain relative bearing measurements, and a particle filter estimator to fuse these measurements with information about the motion of robots throughout time to obtain the desired relative location estimates. A method based on fractional Fourier transform (FrFT) is used to identify and extract sounds of simultaneous chirping robots in the neighbourhood. Furthermore, we evaluate our proposed method in a real world experiment with three simultaneously flying micro air vehicles.**

I. INTRODUCTION

There has been a growing interest in the field of robotics in using multiple autonomous robots for achieving tasks in a collaborative manner. Teams of flying robots can accomplish aerial coverage tasks more robustly and more efficiently compared to a single flying robot. Possible applications include rapidly-deployable communication networks [8], environmental monitoring, aerial surveillance and mapping, traffic monitoring and search and rescue [2]. However, additional challenges are imposed on the design of MAV groups that have so far prevented their use in real missions. Robots within an aerial team are required to interact with each other and to work together towards the achievement of a desired goal. This introduces new problems, such as inter-robot collisions and formation control. A common idea that has been addressed throughout both the natural and artificial swarms literature is that individual's knowledge about the relative location of other swarm members is essential for achieving successful swarming [21, 20, 13] . For example, awareness about the relative range and/or bearing of neighbouring robots can allow a robot to maintain formations [1] [15], and decrease the risk of collisions [3], with other team members.

*This work was supported by a doctoral grant from FCT (SFRH/BD/51070/2010), EC FP-7 research funding mechanism under grant agreement no. 266470 and FCT project [PEst-OE/EEI/LA0009/2011].

[1] Laboratory of Intelligent Systems, Ecole Polytechnique Federale de Lausanne, CH-1015 Lausanne, Switzerland (e-mail: meysam.basiri, felix.schill, dario.floreano@epfl.ch)

[2] Institute for Systems and Robotics, Instituto Superior Tecnico, Lisboa, Portugal (e-mail: pal@isr.ist.utl.pt)

A relative positioning system for a MAV needs to satisfy severe constraints in terms of size, weight, processing power, power consumption, three-dimensional coverage and price. These constraints prevent the current relative positioning systems designed for ground robots and large aerial vehicles to be used in MAVs. Inspired by the sense of hearing in animals [6, 16], which provides them the ability of using sound for communication and localization, we propose an audio based positioning system for MAVs to allow them to obtain information about the position of their local neighbours. Such a system could also possibly be used for perceiving other non-cooperative noise emitting aerial platforms. This paper is organized as follows: Section II describes the related works on relative positioning systems for MAVs. Section III describes the proposed method for our audio based relative positioning system and in Section IV results of real experiments with the proposed method is provided, where three flying MAVs are used in the experiment.

II. STATE OF THE ART

Two main approaches for obtaining relative positioning information in multi-robot systems exist in the literature.

1) Using an absolute positioning system alongside a communication network, allowing robots to obtain relative positioning information by communicating their absolute locations with each other [5] [19]
2) Directly measuring the relative location of other robots using on-board exteroceptive sensors [23] [20]

A drawback with solutions based on the former approach, for relative positioning in MAV swarms, is that an external infrastructure, such as wireless positioning beacons or global positioning system (GPS) satellites, is required for acquiring the absolute positioning information. GPS technologies are vulnerable to jamming and interferences, have low resolution, and are impossible to use in cluttered terrains where there is no direct line of sight with the transmitting satellites [26]. Also, deployment of wireless positioning beacons in the environment in advance of each mission is both costly and time-consuming.

Due to disadvantages of the first approach, much effort has been put into the design of onboard relative positioning systems. In this approach, every individual robot measures the relative position of other robots using onboard exteroceptive sensors. Most current onboard relative positioning systems are developed for ground robots and mainly rely on sensors such as laser range finders, infrared sensors and cameras. However, a relative positioning system for a MAV needs to satisfy constraints in terms of size, weight, processing power, power consumption, three-dimensional coverage and

price. This prevents some of the successful sensor technologies implemented for relative positioning of ground robots to be used in MAVs. Despite this, some effort has been done in transferring these solutions from ground robots to MAVS. Mini laser range finders have been used [25] for detection of large static obstacles (trees and buildings) located in front of a MAV. These sensors provide accurate range measurements of obstacles directly located in front of the laser beam up to a few hundreds of meters away. A major drawback of such sensors is their single point/planar detection ability, which makes them a bad candidate for measuring the position of other MAVs in three-dimensional spaces. Few works also investigate the use of optical sensors for detecting the motion of other aircraft relative to the background scene, computing the relative azimuth and elevation [27]. Systems based on such sensors have a limited field of view and are highly dependent on light conditions and visual contrast. Furthermore, these systems greatly suffer from missed or false detections when the target is located on non-uniform or cluttered backgrounds and also in the presence of vibrations and adverse weather conditions. Small scale Doppler radar transducers are the basis of the sensor suite proposed in [30] for allowing a MAV to detect the presence and measure the relative bearing of colliding obstacles. The sensor suite has a small weight of about 300g and power consumption of 3.7 watts. However, small field of view (30^o), low resolution (15^o) and small range (10m) are some of the major drawbacks of this system. Infrared/ultrasound-based sensor suites have been shown in [23, 22] to provide accurate relative range and bearing estimation in indoor flying platforms. However, they are not suitable sensors for outdoor MAVs due to their short working range.

Hearing has always been one of the key senses among humans and animals allowing them to use sound for attracting attention, communication and localization. Despite this, audition in robotics has not received great attention compared to vision, and most studies on this focus on speech recognition and localization of talkers for home, office, and humanoid robots [14]. In most works, a technique inspired by animal hearing called Inter-aural Time Difference (ITD) (also known as Time Difference of Arrival TDOA) is used for localizing sound sources. This method measures the time delay caused by the finite speed of sound between the signals received by two microphones. While the complex hearing capabilities of animals achieve good performance with only one pair of acoustic sensors, technical systems often use arrays of microphones for assisting robots in locating broadband sound sources in the environment [28].

Audio-based relative positioning for ground robots has not been favoured so far, due to the success of other available sensor technologies and because of the existing challenges in sound source localization inside reverberant and noisy domestic environments. In the case of underwater robotic swarms, the effectiveness of audio based relative positioning compared to other methods have been shown by some researchers [11]. In these systems, a pair of hydrophone sensors onboard a small submarine is used for measuring the relative bearing of other sound emitting submarines.

Audio-based relative positioning for miniature aerial robots has not been addressed so far. However, existing examples in nature show the potential success of such a system for aerial robots. Flight calls of nocturnal migratory birds used for collision avoidance and coordinated migration during night [6], and phonotaxis behaviour among insect swarms for mating and predator avoidance [7] [16] are some of the many existing examples. Furthermore, in a recent work, an acoustic source localization system for MAVs was shown to be effective in locating the source of distress signals on the ground [2]. Design of new acoustic sensors suitable for use on MAVs have been investigated in some recent works [24] [4].

An audio-based relative positioning system for swarm of MAVs will have several advantages. First of all, this system will be based on cheap, small size, passive and omnidirectional sensors which clearly satisfy the constraints of MAVs. The passivity of the sensors will result in low power consumption of the overall system, which is an important parameter for having longer swarm endurance. Also, this system will be independent of illumination and weather conditions, such as fog, dust and rain and will not require direct line-of-sight between robots for its operation. Such a system will also be potentially less computationally expensive compared to vision-based systems, as it will mainly rely on the available phase information in the sound waves rather than the need for extraction of features from sequence of images.

III. Proposed Method

This section explains our method for relative positioning in a group of MAVs. Figure 1 presents the schematic diagram of this system. The overall system is divided in to two main parts of 'Target' and 'Perceiving robots' to illustrate the main units of the system involved at each state. In the target robot state, the robot generates chirps of predefined rate and frequency. In the perceiving state, sound waves are picked up by an on-board microphone array and are continuously checked by the Chirp Detection and Separation unit for existence of chirps in the sound mixture. When a full chirp is detected, it is filtered out from the sound mixture and is then passed to the coherence measuring unit. This unit cross correlates the signals from every microphone pair and obtains a measure of similarity between the signals as a function of time lag applied to one of them. This measure reflects the chirp's time difference of arrival (TDOA) likelihood for all possible time delays. This information along with knowledge of the microphone array's geometry is then used by the Relative Bearing Measurement unit to estimate a measure of the target's direction. Finally, a particle filtering unit is used to estimate more robustly the relative location of the target robot by fusing the noisy bearing measurements with information about the relative motion of robots throughout time. The relative motion between robots are computed using information from the on-board proprioceptive sensors and a communication network. The particle filter is preferred over a parametric approach, such as the Extended Kalman Filter, due to the non-linear nature of the relative

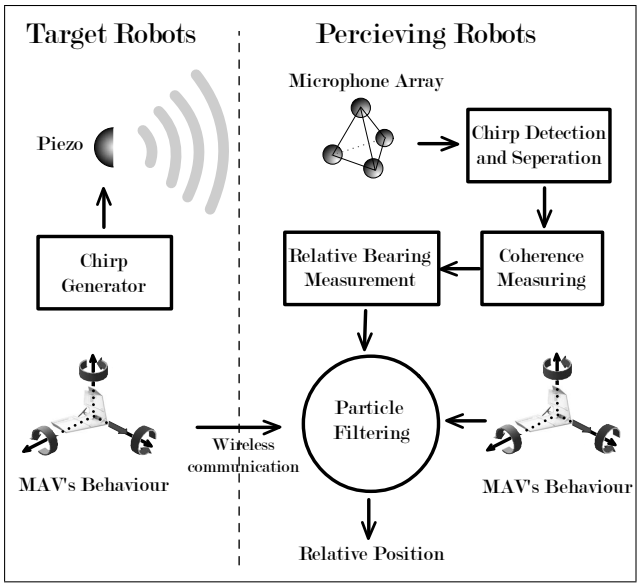

Fig. 1. Schematic diagram of the proposed relative positioning system illustrating main parts of the system

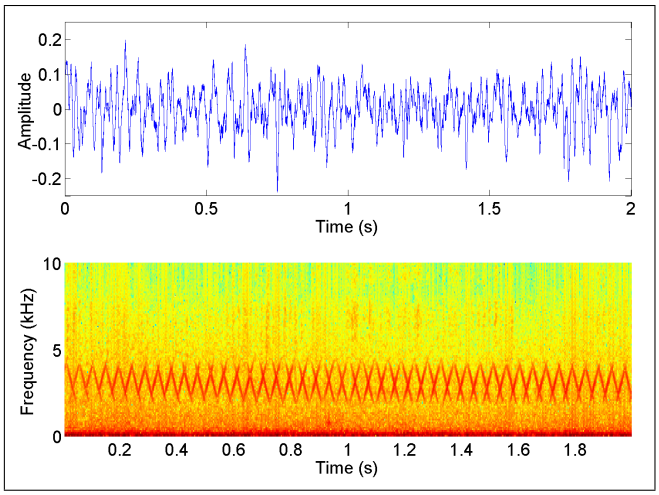

Fig. 2. Sound wave and spectrogram of an in-flight sound recording involving one perceiving robot and two chirping MAVs. The two linear chirps are in the same frequency band and have a different chirp rate.

motion dynamics of the MAVs. A more detailed explanation of each unit is presented in the following sections.

A. Chirp Generator

Piezo transducers are simple, inexpensive and lightweight devices that are suitable to be used on MAVs. These devices generate sound by converting electrical pulses into mechanical vibrations. The resulting sound can be very loud if the frequency of the vibrations are close to the resonance frequency of the piezo element. Hence, in order to generate a loud sound wave that is required here, narrowband sounds such as a pure tone or a band-limited chirp with frequencies close to the resonance frequency should be used. To avoid the problem of ambiguous bearing measurements, caused due to the repetitive nature of pure tone sounds, a band-limited chirp is used for the sound of the targets. The chirp generating unit of every target robot generates periodical linear chirps with a predefined and unique chirp rate. Figure 2 illustrates the sound wave and spectrogram of an in-flight sound recording involving one perceiving robot and two chirping MAVs.

B. Microphone Array

An onboard microphone array is used to simultaneously measure the acoustic field at different points in space. Due to finite speed of sound, incoming sound waves are picked up by the microphones at different time instances. Therefore, by comparing the microphones signals and measuring the time delay among them, it is possible to estimate the direction of arrival of the sound waves (section III-D). A minimum number of four microphones, not all placed on the same plane, is required to localize sounds in 3D-space without ambiguity. Since we are interested in an onboard and real-time system, we only use four microphones here to minimize the computational and hardware loads. Furthermore, a regular tetrahedral microphone array geometry is used to obtain equal localization performance in all directions [9].

C. Chirp Detection and Extraction

This unit is responsible for the detection and extraction of a chirp in the perceived sound wave. The presence of a desired chirp in the sound mixture is initially detected by a template matching technique, where a cross correlation of the sound mixture with a template of the desired chirp is used to find the existence and the time segment containing the chirp. After a chirp is detected, the Fractional Fourier transform (FRFT) [17] of the time window containing the entire chirp is computed with an FRFT order of α obtained by the following equation.

$$\alpha = \frac{2}{\pi}\tan^{-1}(a \times f_s) \tag{1}$$

where f_s is the sampling frequency and a is the chirp rate.

First proposed by Namias [17], FRFT has been recently favoured in the field of signal processing [18], especially when dealing with chirp signals. The FRFT provides a compact representation of the chirp signal allowing us to extract the chirp corresponding to a desired target robot from other sounds. Figure 3 illustrate a comparison between the time, frequency and Fractional domain of a linear chirp signal.

The FRFT, computed by the chirp detection unit, contains an impulse-shaped peak that corresponds to the desired chirp. This chirp is filtered out from other sounds by only retaining the bin with the highest peak along with its few nearby bins and setting all other bins to zero. The ratio of the peak value to the mean value of all zeroed bins prior to zeroing provides a good measure for the quality of the perceived chirp, i.e. signal to noise ratio. This measure is computed and used later as a reliability measure for the obtained bearing measurement. Only measurements satisfying a predefined reliability level are used in the update step of the particle filter. Furthermore, the filtered chirp in the FRFT domain is transformed back to the time domain by computing the inverse FRFT.

D. Coherence measuring

This unit compares the filtered chirp signals of all channels with each other and hence estimates a similarity degree for

every pair of signals as a function of time-lag applied to one of them. Cross correlation is a commonly used technique for measuring the coherence between two signals. Cross correlation of two microphone signals each having a length of N samples can be computed by

$$R_{ij}(\tau) = \sum_{n=0}^{N-1} p_i[n]\, p_j[n-\tau]$$

where $p_i[n]$ is the signal perceived by microphone i and τ is the correlation lag in samples in the range expressed by

$$-\frac{d_m}{c} < \tau < \frac{d_m}{c} \tag{2}$$

where d_m is the distance between the microphones and c is the speed of sound. In order to reduce the computation time, the cross correlation function can be approximated in the frequency domain by computing the inverse Fourier transform of the cross spectrum:

$$R_{ij}(\tau) = \sum_{k=0}^{N-1} P_i[k]\, P_j^*[k] e^{i\frac{2\pi k\tau}{N}} \tag{3}$$

where $P_i(k)$ is the discrete Fourier transform of $p_i(n)$ and P_j^* denotes the complex conjugate of P_j. This results in a reduction of complexity from $O(N^2)$ to $O(N \log N)$, hence making it more suitable for real time computations. A weighting function was introduced into equation (3) by [10] in order to solve the problem of wide cross correlation peaks.

$$R_{ij}(\tau) = \sum_{k=0}^{N-1} \frac{P_i[k]\, P_j^*[k]}{|P_i[k]|\,|P_j[k]|} e^{i\frac{2\pi k\tau}{N}} \tag{4}$$

This weighting function whitens the cross-spectrum of the signals allowing equal contribution of all frequencies in estimating the cross correlation and resulting in sharper peaks. This is only suitable when the desired sound is broadband,

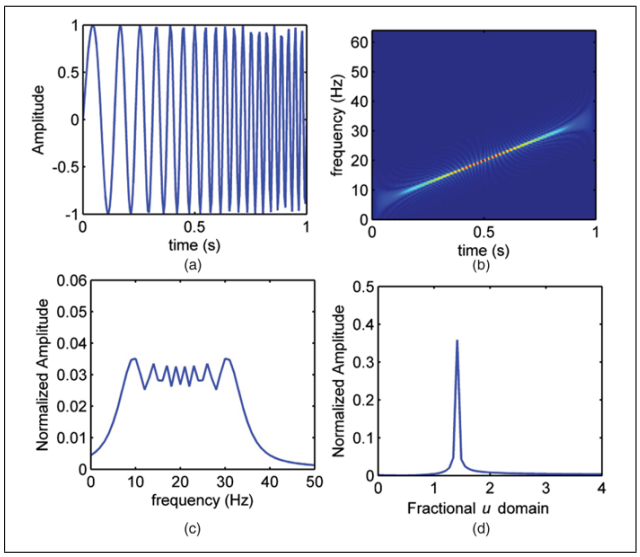

Fig. 3. A comparison between the time, frequency and Fractional domain of a linear chirp. a) Time domain b) Spectrogram c) Frequency domain d) Fractional domain

but for narrowband sounds it amplifies the background noise. Therefore, a modified version of equation (4) was used here instead to solve this problem.

$$R_{ij}(\tau) = \sum_{k=0}^{N-1} \chi \left[\frac{P_i P_j^*}{|P_i|\,|P_j|}\right] e^{i\frac{2\pi k\tau}{N}} \tag{5}$$

where

$$\chi = \begin{cases} 1 & f_{\min} < f < f_{\max} \\ 0 & \text{otherwise} \end{cases}$$

and $f_{\min}$ and $f_{\max}$ are the minimum and maximum frequencies of the chirp.

E. Relative Bearing measurement

After obtaining $R_{ij}(\tau)$ from (5) for all microphone pairs ij, the Relative Bearing Measurement unit searches for the most likely sound source direction $\overrightarrow{b}_m$

$$\overrightarrow{b_m} = \arg\max_{\vec{b}} \sum_{i,j} R_{ij}(\tau_{\vec{b}ij}) \tag{6}$$

where time delay $\tau_{\vec{b}ij}$ corresponds to direction $\overrightarrow{b}$ and is computed from the coordinates of microphones i and j in the body fixed coordinate system. In this work a full direction grid search for all directions $\overrightarrow{b}$ around the robot is used for finding $\overrightarrow{b_m}$. Other search methods exist in the literature that can reduce the cost of this search if necessary [29].

F. Particle Filtering

The previous sections described methods of providing an instantaneous noisy information about the relative bearing of a target robot in the neighbourhood. This information is combined with the relative motion dynamics of the perceiving and the target MAVs, measured by onboard interoceptive sensors, using a particle filter to recursively estimate the probability density of the target location.

At time instant t, the relative position of a single target robot is modelled using a set of N particles of vectors p_i and weight w_i, where $p_i = (p_{xi}, p_{yi}, p_{zi})$ is a vector in the body-fixed coordinate system of the perceiving robot that starts at its origin and ends at a point in space. p_i can also be described in the body-fixed spherical coordinate system $(\angle\phi, \angle\theta, r)$ by:

$$u_i = (\phi_i, \theta_i, r_i) \qquad i = 1, 2, ..N \tag{7}$$

where ϕ_i is the relative azimuth defined in the range $[-\pi, \pi]$, θ_i is the relative elevation defined in the range $[-\pi/2, \pi/2]$ and r_i is the relative range defined in the range $[R_{min}, R_{max}]$. R_{min} and R_{max} are dependent on the platform size and the sound power respectively. For the MAVs and the piezos that are used in this work the ranges are found approximately to be $[1, 250]$ meters.

A three dimensional state vector is specified for every particle:

$$S_i(t) = [\phi_i(t)\ \ \theta_i(t)\ \ r_i(t)] \tag{8}$$

The algorithm starts by forming an initial set of particles $\{S_i(0), i = 1 : N\}$ for every target robot detected to be in the

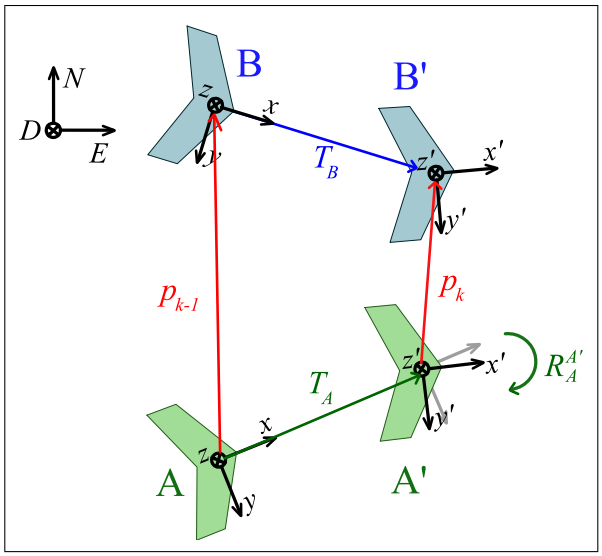

Fig. 4. Positions of two robots (perceiving A and target B) in two successive time steps along with coordinate systems and connecting vectors

neighbourhood. Particles either could be generated uniformly over the entire state space, or only over a desired part of the state space if some prior knowledge about the possible location of the target is available. In this work, the initial state space is reduced to all vectors in the space having a small deviation from the first reliable bearing measurement.

Particle filters consists of two main steps at each iteration: Prediction and Update.

1) Prediction: In the prediction step, a set of new particles $\tilde{S}_i(t)$ is predicted by propagating $S_i(t-1)$ according to a probabilistic relative motion model. This model is derived with the assumption that, at every time step, robots have a forward motion, (i.e. along the x axis of their body-fixed coordinate system), followed by a three dimensional rotation, (i.e. yaw (λ), pitch (β) and roll (α) rotations around the z, y and x axis of the body fixed coordinate system respectively). Figure 4 illustrates the positions of two robots in two successive time steps consisting of a perceiving robot (Robot A) and a target robot (Robot B). Using linear algebra the following relationship between the vectors can be described:

$$\overrightarrow{p}_k = R_{B'}^{A'}(R_B^{B'}\overrightarrow{T}_B) + R_A^{A'}\overrightarrow{p}_{k-1} - R_A^{A'}\overrightarrow{T}_A \tag{9}$$

where R_I^J is a rotation matrix that rotates a vector from the coordinate system I to the coordinate system J:

$$R_I^J = R_z(\lambda_J - \lambda_I).R_y(\beta_J - \beta_I).R_x(\alpha_J - \alpha_I) \tag{10}$$

$(\lambda_I, \beta_I, \alpha_I)$ is the bearing of the coordinate system I relative to a fixed NED coordinate system and (R_z, R_y, R_x) are basic rotation matrices that rotate vectors about the local z, y and x axis respectively.

Equation (9) is used by the perceiving robot to predict the particles $\overrightarrow{\tilde{p}}_{ki}$ from their previous values $\overrightarrow{p}_{(k-1)i}$. For this, speed and orientation of the perceiving robot, and of the target robot transmitted via a communication network, are used. The forward motion vectors $\overrightarrow{T}_A$ and $\overrightarrow{T}_B$ are initially computed from the speed sensor readings $V_{A(k-1)}$ and $V_{B(k-1)}$ at time $k-1$

$$\overrightarrow{T}_A = \begin{bmatrix} (V_{A(k-1)} + \xi_V)dt \\ 0 \\ 0 \end{bmatrix} \quad \overrightarrow{T}_B = \begin{bmatrix} (V_{B(k-1)} + \xi_V)dt \\ 0 \\ 0 \end{bmatrix}$$

where dt is the time interval between the two time steps and $\xi_V = N(0, \sigma_V)$ is a random number generated with a normal distribution of mean zero and standard deviation σ_V. The value of σ_V is chosen in relation with the reliability in the speed sensor reading measurements. Furthermore, the rotation matrices $R_I^J(\lambda + \xi_\lambda, \beta + \xi_\beta, \alpha + \xi_\alpha)$ in equation (9) are computed from the bearing measurements $(\lambda, \beta, \alpha)_{I,J}$ and using equation (10), with $\xi_\lambda = N(0, \sigma_\lambda)$, $\xi_\beta = N(0, \sigma_\beta)$ and $\xi_\alpha = N(0, \sigma_\alpha)$ to consider the noise in the measurements. Finally, equation (9) can be solved for the prediction $\overrightarrow{\tilde{p}}_{ki}$ of particle i.

2) Update: As previously explained, an audio based relative bearing measurement is obtained at every time-step. In the update step, the likelihood of obtaining these measurements is investigated for every particle and particles are weighted according to this measure. For this investigation, we propose the likelihood function:

$$w_i = \frac{1}{\sigma_m\sqrt{2\pi}} e^{-\frac{1}{2}\left(\frac{\varepsilon_i}{\sigma_m}\right)^2} \tag{11}$$

where

$$\varepsilon_i = \angle(\overrightarrow{b}_{mk}, \overrightarrow{\tilde{p}}_{ki}) \tag{12}$$

is the angle between the measured bearing $\overrightarrow{b}_{mk}$ at time k and the predicted vector $\overrightarrow{\tilde{p}}_{ki}$ of particle i. The value of σ_m reflects the confidence of the bearing measurements and is found empirically. As mentioned in section III-C, only reliable measurements obtained from chirps that have a good signal to noise ratio, i.e. that satisfy the predefined reliability level, is used in the update step and this step is skipped otherwise.

Note that, the likelihood function (11) is formed by assuming that the angular error between the direction measurements $\overrightarrow{b}_m$ and the true directions $\overrightarrow{b}_T$, have a Gaussian distribution with mean zero and standard deviation σ_m. i.e.

$$\angle(\overrightarrow{b}_m, \overrightarrow{b}_T) \sim \mathcal{N}(0, \sigma_m^2) \tag{13}$$

Experiments show that this assumption is a reasonable assumption. Figure 6 shows the relative bearing measurements and the histogram of the angular errors from a field experiment involving a target robot and a perceiving robot.

3) Relative Position Estimation: The relative range and bearing of the target can be estimated at each time step from the probability density function represented by a particle set. For this, a weighted mean of all particles' positions could be employed. However, to avoid inaccurate estimations for situations with multi-modal distributions, a weighted mean of particles located in a local neighbourhood of the particle with the highest weight is used instead:

$$\bar{S}_T = \sum_{i=1}^{K} w_i S_i : \forall\, |S_i - S_{max}| < \xi \tag{14}$$

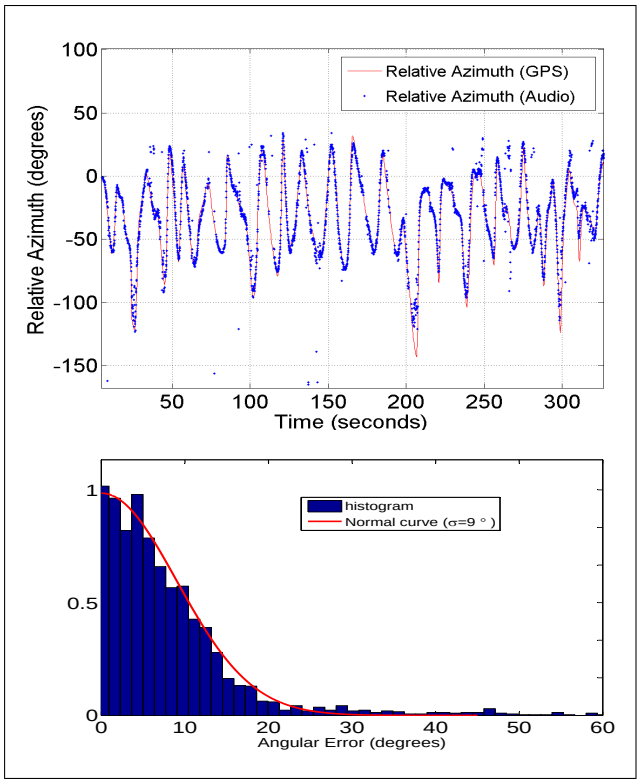

Fig. 5. Audio based bearing measurements from an experiment involving a perceiving robot and a target robot. In this experiment, the perceiving robot was fixed over the ground to eliminate the uncertainties, in the estimation of the true bearings, caused by the oboard gyros and the GPS of the perceiving robot. The target robot is flown manually in proximity of the perceiving robot and its onboard GPS is used only to compute the true bearings. top: Audio based and GPS based relative azimuth measurements. bottom: histogram of the angular errors between the measured bearings and the true bearings.

Finally, the particles are resampled according to their normalized weights to avoid the problem of degeneracy of the particle filtering algorithm.

IV. Experiments and Results

To test and verify the proposed algorithm, multiple real experiments were performed with three similar MAV platforms such as the one shown in figure 6. A microphone array consisting of four microphones is mounted on one of the robots along with a digital sound recorder for recording the microphone signals. The microphones are covered with wind protection and are positioned in a way to form a regular tetrahedron of edge length 10 cm. This dimension was selected relative to the size of the MAV to prevent the drag caused by the microphones from affecting the MAV's stability. Audio is recorded with a sampling rate of 48kHz. The two target robots are equipped with a piezo transducer and a micro controller programmed to generate periodic linear chirps as shown in figure 2. One of the robots produce chirps with up-sweep frequency from 1700kHz to 4700kHz and the other robot have chirps with down-sweep frequency from 4700kHz to 1700kHz. The rate of chirping for both robots are set to about 20 chirps per second with each chirp having a duration of approximately 0.05 seconds.

Fig. 6. Picture of the MAV platform [12] used for experimenting the proposed algorithm. Four microphones and an on-board digital sound recorder is used for recording sounds during flight.

All MAVs are equipped with an autopilot that allows it to fly fully autonomously to predefined waypoints. The orientation, altitude, air-speed and global positioning information of the MAVs are measured using on-board sensors and are transmitted and recorded on a ground station. The roll and pitch orientations of the MAVs are measured using on-board gyroscopes and since no compass is currently present on the MAVs, the heading information was obtained from the on-board GPS sensor. The MAVs were controlled to fly within the visual range of a safety pilot while the engine power of the perceiving robot was occasionally reduced or even turned off to increase the detection range by increasing the signal to noise ratio. This reduction in the engine power is achieved automatically whenever the MAV is descending.

Figure 7 shows the path of all three robots, recorded by the GPS sensors, for 25 seconds duration of flight time. The relative azimuth estimations for this duration of time is shown in Figure 8. These estimates are compared against the relative azimuth values computed from the GPS positions and the onboard IMU data and show a good correspondence at all times. Furthermore, the reliable bearing measurements, obtained by the Relative Bearing Estimation unit, and the perceiver's motor input is illustrated in this figure. It is shown that for high motor inputs fewer reliable measurements are obtained. This is due to the loudness of the self-propeller noise

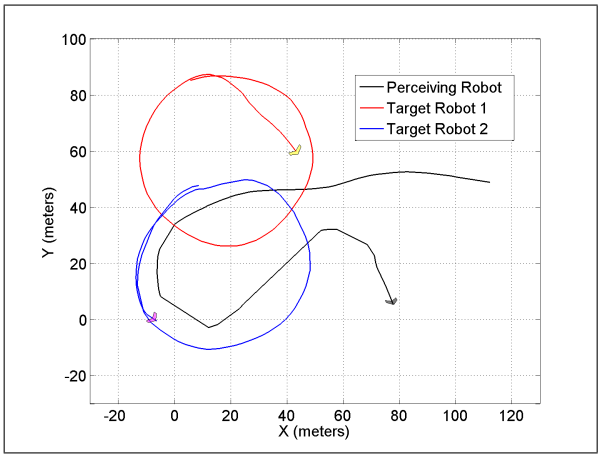

Fig. 7. The motion path of robots recorded by onboard GPS sensors, for 25 seconds of flight time in an experiment involving one perceiving robot to locate and track two target robots

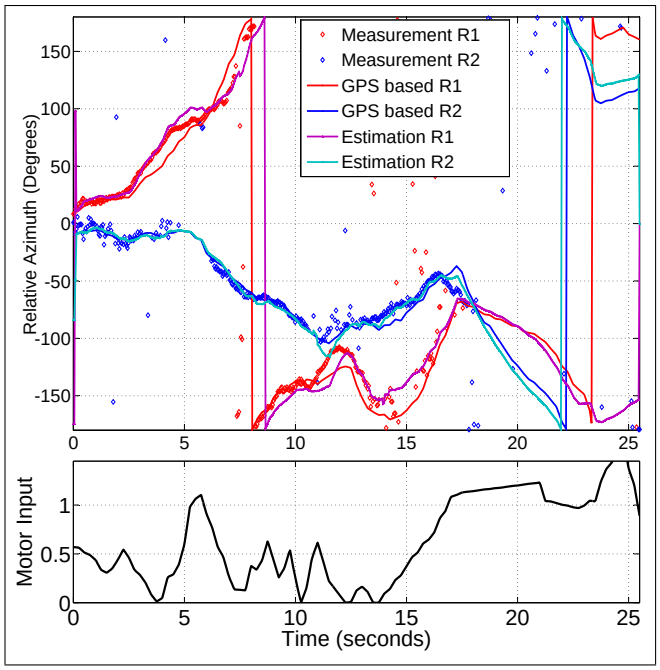

Fig. 8. top: The relative azimuth estimations from the Particle Filtering unit compared with the relative azimuth computed from the GPS positions and the onboard IMU orientations. The relative azimuth measurements obtained by the Relative Bearing Measurement unit are shown by small markers. bottom: Motor input of the perceiving robot

which affects the signal to noise ratio. Despite this, the relative bearing of the targets are shown to be tracked correctly long after observations are no longer available.

The relative range estimations along with the particle distributions and GPS based range estimates are shown in Figure 9. It can be seen that, the particles gradually converge towards the correct relative range and furthermore track it with an acceptable accuracy. As expected, the speed of convergence and the accuracy in the relative range estimations are dependent on the motions and positions of the robots. For some types of relative motions, the particles having an inaccurate range are eliminated faster than for other types of motions. Figure 9 shows that in the first few seconds, where the perceiving robot is further away from the target robots, and robots are moving towards each other, particles are still widely spread in relative range although they have converged to the correct bearing. As the robots get closer and pass each other, the disparity of the particles is reduced.

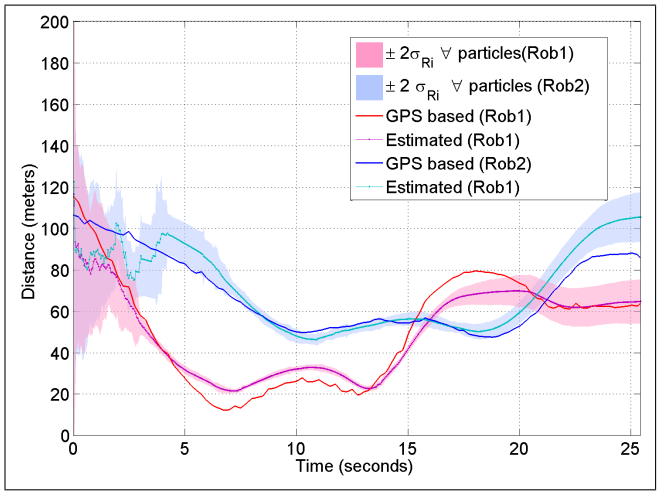

Fig. 9. The Relative range estimations, standard deviation of the relative range of all particles and GPS based range values

V. Conclusion and Future Work

This paper presents a solution to the problem of relative positioning for a group of micro air vehicles. The solution provided in this paper requires MAVs to be equipped with an on-board microphone array to measure the relative bearing to other sound emitting MAVs and on-board sensors to obtain information about the state of the MAVs. The particle filtering technique used in this paper was shown to be well-suited for fusing the relative bearing measurements with relative motion of the MAVs in order to achieve robust estimation of the relative range and bearing. In this work a communication network between the robots was required to share sensor informations and compute the relative motion between the robots. Removing the need of a communication network, by considering some prior knowledge about the behaviours of the robots, is an area of work we are currently pursuing. In this work a piezoelectric transducer was used on the robots as the target source. However as the engine of nearly all flying platforms generate sound when flying, this sound could possibly be used in the future for detecting other non-cooperative robots and aerial platforms.

References

[1] M. Basiri, A.N. Bishop, and P. Jensfelt. Distributed control of triangular formations with angle-only constraints. *Systems & Control Letters*, 59(2):147–154, 2010.

[2] M. Basiri, F. Schill, P.U. Lima, and D. Floreano. Robust acoustic source localization of emergency signals from micro air vehicles. In *2012 IEEE/RSJ International Conference on Intelligent Robots and Systems (IROS)*, pages 4737 –4742, oct. 2012. doi: 10.1109/IROS.2012.6385608.

[3] R. Carnie, R. Walker, and P. Corke. Image processing algorithms for uav "sense and avoid". In *IEEE International Conference on Robotics and Automation (ICRA)*, pages 2848 –2853, may 2006. doi: 10.1109/ROBOT.2006.1642133.

[4] HE de Bree, Ir Jelmer Wind, Ir Erik Druyvesteyn, and H te Kulve. Multi purpose acoustic vector sensors for battlefield acoustics. In *Proceedings of the DAMA Conference*, 2010.

[5] P. DeLima, G. York, and D. Pack. Localization of ground targets using a flying sensor network. In *IEEE International Conference on Sensor Networks, Ubiquitous, and Trustworthy Computing*, volume 1, page 6 pp., june 2006. doi: 10.1109/SUTC.2006.1636176.

[6] A. Farnsworth. Flight calls and their value for future ornithological studies and conservation research. *The Auk*, 122(3):733–746, 2005.

[7] G. Gibson, B. Warren, and I.J. Russell. Humming in tune: sex and species recognition by mosquitoes on the wing. *JARO-Journal of the Association for Research in Otolaryngology*, 11(4):527–540, 2010.

[8] S. Hauert, S. Leven, J.C. Zufferey, and D. Floreano. Communication-based swarming for flying robots. In *Proc. Intl. Conf. Robotics and Automation Workshop on Network Science and Systems*, 2010.

[9] Jwu-Sheng Hu, Chieh-Min Tsai, Chen-Yu Chan, and Yung-Jung Chang. Geometrical arrangement of microphone array for accuracy enhancement in sound source localization. In *Control Conference (ASCC), 2011 8th Asian*, pages 299–304. IEEE, 2011.

[10] C. Knapp and G. Carter. The generalized correlation method for estimation of time delay. *IEEE Transactions on Acoustics, Speech and Signal Processing*, 24(4):320–327, 1976.

[11] N. Kottege and U.R. Zimmer. Relative localisation for auv swarms. In *Symposium on Underwater Technology and Workshop on Scientific Use of Submarine Cables and Related Technologies, 2007.*, pages 588–593. IEEE, 2007.

[12] S. Leven, J.C. Zufferey, and D. Floreano. A simple and robust fixed-wing platform for outdoor flying robot experiments. In *International symposium on flying insects and robots*, pages 69–70, 2007.

[13] Maja J. Mataric. Behaviour-based control: examples from navigation, learning, and group behaviour. *Journal of Experimental and Theoretical Artificial Intelligence*, 9(2-3):323–336, 1997. doi: 10.1080/095281397147149.

[14] Y. Matsusaka, T. Tojo, S. Kubota, K. Furukawa, D. Tamiya, K. Hayata, Y. Nakano, and T. Kobayashi. Multi-person conversation via multi-modal interface-a robot who communicate with multi-user. In *Sixth Eu Conference on Speech Communication and Technology*, 1999.

[15] N. Moshtagh, N. Michael, A. Jadbabaie, and K. Daniilidis. Vision-based, distributed control laws for motion coordination of nonholonomic robots. *IEEE Transactions on Robotics*, 25(4):851 –860, aug. 2009. ISSN 1552-3098. doi: 10.1109/TRO.2009.2022439.

[16] P. Muller and D. Robert. A shot in the dark: the silent quest of a free-flying phonotactic fly. *Journal of Experimental Biology*, 204(6):1039–1052, 2001.

[17] V. Namias. The fractional order fourier transform and its application to quantum mechanics. *IMA Journal of Applied Mathematics*, 25(3):241–265, 1980.

[18] H.M. Ozaktas, B. Barshan, D. Mendlovic, and L. Onural. Convolution, filtering, and multiplexing in fractional fourier domains and their relation to chirp and wavelet transforms. *Journal of the Optical Society of America*, 11(2):547–559, 1994.

[19] D. Pack, G. York, and R. Fierro. Information-based cooperative control for multiple unmanned aerial vehicles. In *Proceedings of the 2006 IEEE International Conference on Networking, Sensing and Control, ICNSC*, pages 446 –450, 0-0 2006. doi: 10.1109/ICNSC.2006.1673187.

[20] J. Pugh and A. Martinoli. Relative localization and communication module for small-scale multi-robot systems. In *Proceedings IEEE International Conference on Robotics and Automation, ICRA*, pages 188 –193, may 2006. doi: 10.1109/ROBOT.2006.1641182.

[21] Craig W. Reynolds. Flocks, herds and schools: A distributed behavioral model. *SIGGRAPH Comput. Graph.*, 21(4):25–34, August 1987. ISSN 0097-8930. doi: 10.1145/37402.37406.

[22] F. Rivard, J. Bisson, F. Michaud, and D. Létourneau. Ultrasonic relative positioning for multi-robot systems. In *IEEE International Conference on Robotics and Automation, ICRA.*, pages 323–328. IEEE, 2008.

[23] J.F. Roberts, T.S. Stirling, J.-C. Zufferey, and D. Floreano. 2.5d infrared range and bearing system for collective robotics. In *IEEE/RSJ International Conference on Intelligent Robots and Systems, IROS*, pages 3659 –3664, oct. 2009. doi: 10.1109/IROS.2009.5354263.

[24] F. Ruffier, S. Benacchio, F. Expert, and E. Ogam. A tiny directional sound sensor inspired by crickets designed for micro-air vehicles. In *Sensors, 2011 IEEE*, pages 970–973. IEEE, 2011.

[25] Jeffery B Saunders, Brandon Call, Andrew Curtis, Randal W Beard, and Timothy W McLain. Static and dynamic obstacle avoidance in miniature air vehicles. *AIAA Infotech at Aerospace*, 2005.

[26] R. Siegwart and I.R. Nourbakhsh. *Introduction to autonomous mobile robots*. MIT press, 2004.

[27] J. Utt, J. McCalmont, and M. Deschenes. Development of a sense and avoid system. *AIAA Infotech at Aerospace*, 2005.

[28] J.M. Valin, F. Michaud, J. Rouat, and D. Létourneau. Robust sound source localization using a microphone array on a mobile robot. In *IEEE/RSJ International Conference on Intelligent Robots and Systems , IROS*, volume 2, pages 1228–1233. IEEE, 2003.

[29] J.M. Valin, F. Michaud, and J. Rouat. Robust localization and tracking of simultaneous moving sound sources using beamforming and particle filtering. *Robotics and Autonomous Systems*, 55(3):216–228, 2007.

[30] A. Viquerat, L. Blackhall, A. Reid, S. Sukkarieh, and G. Brooker. Reactive collision avoidance for unmanned aerial vehicles using doppler radar. In *Field and Service Robotics*, pages 245–254. Springer, 2008.